Pergamon

PII: S0191-8141(96)00077-6

Journal of Structural Geology, Vol. 19, No. 1, pp. 113 to 127, 1997

0191-8141/97 $17.00 + 0.00

The fabric attractor

C. W. PASSCHIER

Institut für Geowissenschaften, Universität Mainz, 55099, Mainz, Germany

(*Received* 21 *March* 1996; *accepted in revised form* 10 *September* 1996)

Abstract—The nature of fabric accumulation in high strain zones such as ductile shear zones depends on the nature and orientation of flow eigenvectors or apophyses. Some flow apophyses can act as 'attractors' of material lines or principal finite strain axes. This paper explains the nature of such attractors and discusses their significance and orientation in different monoclinic flow types. In ductile shear zones, strain values are high enough to show the effect of attractors in deformed rocks clearly. The concept of attractors can be used in deformation modelling, and can help in understanding the accumulation of deformation fabrics in homogeneous and inhomogeneous flow, e.g. around boudins, mantled porphyroclasts and sheath folds.

INTRODUCTION

The influence of flow geometry on the form of fabrics in deformed rocks has been a subject of interest in the earth sciences for a number of years. The geometry of flow is easily described by the nature and orientation of eigenvectors of the flow tensor and a classification of flow by the nature of its eigenvectors can help to understand the development of fabrics in rocks.

The exact relation between flow parameters such as vorticity, volume change rate or dilation rate and deformation geometry can be very complicated at low finite strain or if flow parameters changed significantly in the course of the deformation history. If changes were small and finite strain is high, however, the geometry of deformation fabrics may reflect the bulk geometry of flow. Such circumstances are found in many ductile shear zones.

In studies of fabric development in ductile shear zones, simple shear flow is a commonly used model, and development of fabrics by this flow type is relatively well understood. Since simple shear is an oversimplification in many cases, it is interesting to investigate the consequences of other non-coaxial three-dimensional flow types for the accumulation of fabrics in shear zones. In order to do this, a general facilitating concept is introduced in the form of 'attractors'. The attractor concept is a generalisation of the idea of 'blocked positions' or 'sinks' of rigid objects and material lines and planes mentioned in older work such as Passchier (1987), Fossen (1993) and Fossen *et al.* (1994). This paper discusses several types of attractors such as attractors of material lines, of finite strain axes and of fabric elements such as crystallographic axes. In order to explain the attractor concept, some aspects of three-dimensional flow and progressive deformation must be outlined in detail.

FLOW TYPES

Flow, a description of the velocity of particles, is homogeneous if its properties are the same throughout a deforming volume of material. Here, mainly homogeneous flow is treated because its mathematical description is simple and straightforward and forms a basis for discussion of the myriad of possible types and sequences of heterogeneous flow and progressive deformation. Heterogeneous flow can usually be modelled by subdivision of the deforming continuum into domains of homogeneous flow.

In the case of homogeneous flow, material lines rotate and stretch but remain straight. It is therefore possible to describe homogeneous flow in terms of the stretching rate and the rate and direction of rotation of the set of all material lines in a deforming body (Passchier, 1990, 1991). In any type of homogeneous flow, three directions exist in which maximum, intermediate and minimum stretching rate of material lines are realised (Fig. 1). These spatial axes are orthogonal in any flow type and are known as the instantaneous stretching axes (ISA) **a, b** and **c** (Fig. 1; Passchier, 1990, 1991) with principal instantaneous stretching rates *a, b* and *c* (Fig. 1). *a, b* and *c* can have any magnitude but in this paper, $b > c$ by definition in order to avoid treatment of flow types that are each other's mirror image. Flow types can be separated into two major groups: *coaxial*, in which material lines parallel to ISA do not rotate with respect to these axes; and *non-coaxial*, in which they do. Any non-coaxial flow type can be derived from a coaxial flow type by addition of a rigid-body rotation component to all material lines, keeping ISA irrotational in an external reference frame (Means *et al.*, 1980; Lister and Williams, 1983; Passchier, 1990, 1991). This rigid-body rotation component with respect to ISA is known as the vorticity of the flow. The orientation and magnitude of the vorticity can be defined by a single vector **w** (Fig. 1).

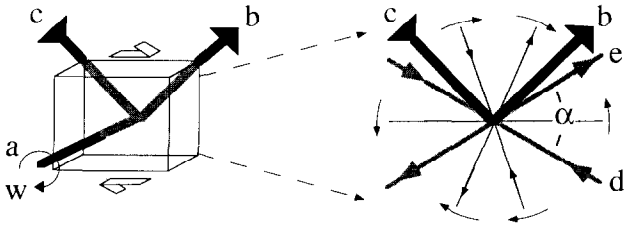

Fig. 1. Schematic illustration of homogeneous monoclinic flow as defined in this paper. Instantaneous stretching axes (ISA) **a**, **b** and **c** are shown as bold black lines. The vorticity vector **w** is parallel to **a**. The *b*-*c* plane is shown highlighted at right; the sense of rotation and stretching of some material lines (thin lines) with respect to ISA (bold black lines) is indicated. Bold grey lines **e** and **d** are flow apophyses. All material lines rotate with respect to ISA except lines parallel to the apophyses; these may stretch but do not rotate.

Material lines that do not rotate with respect to ISA are not exclusively found in coaxial flow types; they may also occur in non-coaxial flows, but are not all parallel to ISA in that case. In any flow type, the spatial axes parallel to such irrotational material lines are known as flow eigenvectors. Since the term eigenvectors can also be used for irrotational lines in certain components of the flow or for deformation, the term *flow apophyses* is used here specifically for eigenvectors of flow in a reference frame where ISA are not rotating (Fig. 1; Ramberg, 1975; Passchier, 1988). Flow apophyses need not be orthogonal and are usually inclined to ISA (Fig. 1).

Strictly speaking, the geometry of all types of homogeneous flow with ISA fixed in an external reference frame can be fully described by six numbers, e.g. the principal stretching rates and the components of the vorticity vector. However, if we wish to describe flow in a geological or experimental context, the orientation of ISA with respect to some external reference frame, e.g. the Earth's surface or the symmetry axes of an experimental rig, should be given. For this purpose, three more numbers are needed in a general case. In all, nine numbers are therefore required in the most general case to describe flow in a volume of material in three dimensions: this is the number of coefficients in a 3×3 velocity gradient matrix commonly used to describe flow (Malvern, 1969).

General flows are difficult to handle because of the nine numbers that are required for a full description: it is obviously difficult to show the effect of nine independent variables on development of structures in graphs. In the following sections a reduced, special type of flow is treated which can be defined by just four numbers. This is attained by ignoring the three numbers reserved for description of flow in an external reference frame, and by fixing the orientation of the vorticity vector **w** parallel to **a**, one of the ISA (Fig. 1). Flow of this type has a monoclinic or (in special cases) higher symmetry; in this paper it is referred to as *monoclinic flow*.

Obviously, the use of a flow type with just four independent parameters is inspired by mathematical simplicity, but there is also a practical reason to restrict treatment to monoclinic flows. In a shear zone with planar wall rocks in an originally isotropic material, the orientation of the stress field in the zone will not only determine the orientation of ISA, but also that of the vorticity vector (Weijermars, 1991). The vorticity vector will lie approximately orthogonal to the instantaneous stretching axis with the smallest (usually negative) stretching rate (**c** in Fig. 1), and in the plane of the shear zone. As a result, the vorticity vector in planar ductile shear zones can be expected to lie close to parallelism with **a** in the plane of the shear zone. The fact that most shear sense indicators in ductile shear zones have a monoclinic or higher shape symmetry with the symmetry axis normal to the displacement direction and in the plane of the shear zone seems to support this line of reasoning (Passchier and Trouw, 1995; Hanmer and Passchier, 1991). Robin and Cruden (1994) modelled shear zones with a complex, inhomogeneous flow pattern and found local triclinic flow symmetry in their model, but even in their example deviation from monoclinic flow is small.

The four parameters that fully describe monoclinic flow are a, b, c and w where w is the length of the vorticity vector (Fig. 1). The geometry of flow defined by these parameters is dependent on their relative, but not their absolute, magnitudes: for example, the geometry of flow in a magma and in solid rocks may be identical, but a, b, c and w in each flow may differ by several orders of magnitude. It is therefore useful to define normalised rather than absolute parameters.

Normalisation of flow parameters can be realised by defining some mean stretching rate $\dot{s}$, and dividing flow parameters by this number. There is a large number of possible combinations, but for reasons outlined below a mean stretching rate was chosen that only depends on parameters a and c in the plane normal to the vorticity vector:

$$\dot{s} = \frac{b - c}{2}. \tag{1}$$

Three normalised numbers can now be defined:

$$W_n = \frac{w}{2\dot{s}} = \frac{w}{b - c} \quad \text{(the sectional kinematic vorticity number)}, \tag{2}$$

$$A_n = \frac{b + c}{2\dot{s}} = \frac{b + c}{b - c} \quad \text{(the sectional kinematic dilatancy number)}, \tag{3}$$

$$T_n = \frac{a}{2\dot{s}} = \frac{a}{b - c}. \tag{4}$$

These three normalised parameters are dimensionless and fully describe the geometry of flow. The mean stretching rate $\dot{s}$ only defines the rate at which flow occurs; it carries no information on the *geometry* of homogeneous flow and does not influence the geometry of homogeneous deformation. Effectively, three numbers are therefore sufficient to completely define monoclinic flow types; this is useful, since it means that three-

dimensional graphs or their projections can be used to illustrate flow geometries.

Two of the numbers defined above have been used in other papers: W_n (Passchier, 1988, 1990, 1991; Robin and Cruden, 1994) and A_n (Passchier, 1990, 1991). W_n defines the degree of rotationality of the flow type and is defined to be positive for a sinistral shear sense and negative for a dextral shear sense in the orientation of Fig. 1, in accordance with the orientation of the vorticity vector. A_n defines the relative area-change rate in the *b–c* plane. T_n defines the rate of stretch along **a**. Figure 2 shows some deformed cubes that illustrate the meaning of W_n, A_n and T_n for flow and progressive deformation.

W_n as used in this paper, in Passchier (1988, 1990, 1991) and Robin and Cruden (1994), is a sectional kinematic vorticity number and differs from the kinematic vorticity number W_K defined by Truesdell (1954) and Means *et al.* (1980):

$$W_K = \frac{w}{\sqrt{2(a^2 + b^2 + c^2)}}. \quad (5)$$

W_K is related to W_n as used in this paper by:

$$W_n = W_K\sqrt{2T_n^2 + A_n^2 + 1}. \quad (6)$$

If T_n and A_n are zero (plane strain flow without area change), both kinematic vorticity numbers are equal. Another useful number derived from A_n and T_n is:

$$V_n = \frac{a+b+c}{2\dot{s}} = \frac{a+b+c}{b-c} = T_n + A_n. \quad (7)$$

V_n describes the relative rate of volume change of a flow type: for isochoric flows (no instantaneous volume change) it is zero.

FLOW IN TWO AND THREE DIMENSIONS

It is generally difficult to present the three-dimensional geometry of the vector field of flow in diagrams. In homogeneous flow, however, straight lines remain straight and all material lines that constitute a plane will therefore remain part of that plane, even though the plane itself may be rotating. It is therefore possible to use two-dimensional cross-sections through three-dimensional flow to illustrate its geometry.

As outlined by Passchier (1991), all two-dimensional flow types can be presented as a simple function of W_n and A_n for the plane of observation, where the former refers to a vorticity vector component normal to that plane. In three-dimensional monoclinic flow, one apophysis is parallel to **a** and to the vorticity vector **w**, and up to two apophyses, **d** and **e**, lie in the *b–c* plane, symmetrically arranged with respect to **b** and **c** (Fig. 1). The *b–c* plane is therefore particularly useful as a section to show flow geometry, as outlined below.

Figure 3 illustrates how flow types in the *b–c* plane differ as a function of W_n and A_n. The flow types are represented by sets of curves that are parallel to velocity vectors in the flow field (streamlines). The streamlines also coincide with paths that particles follow in progres-

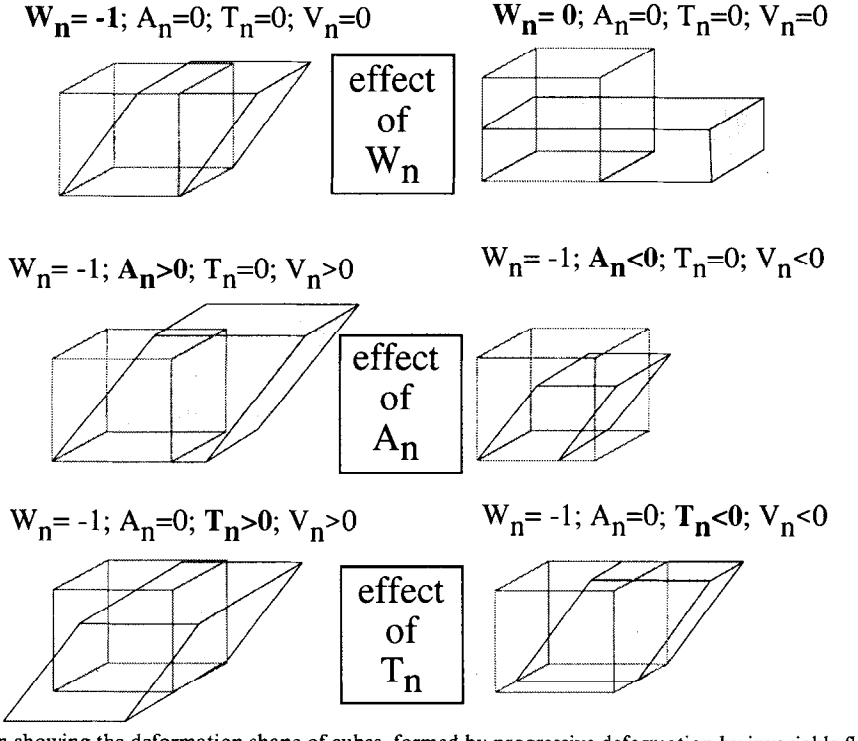

Fig. 2. Cartoon showing the deformation shape of cubes, formed by progressive deformation by invariable flow types with parameters as listed. Although this figure shows finite deformation and not flow, it serves to illustrate the physical significance of the numbers W_n, A_n, T_n and V_n and their individual effects on flow and deformation geometry.

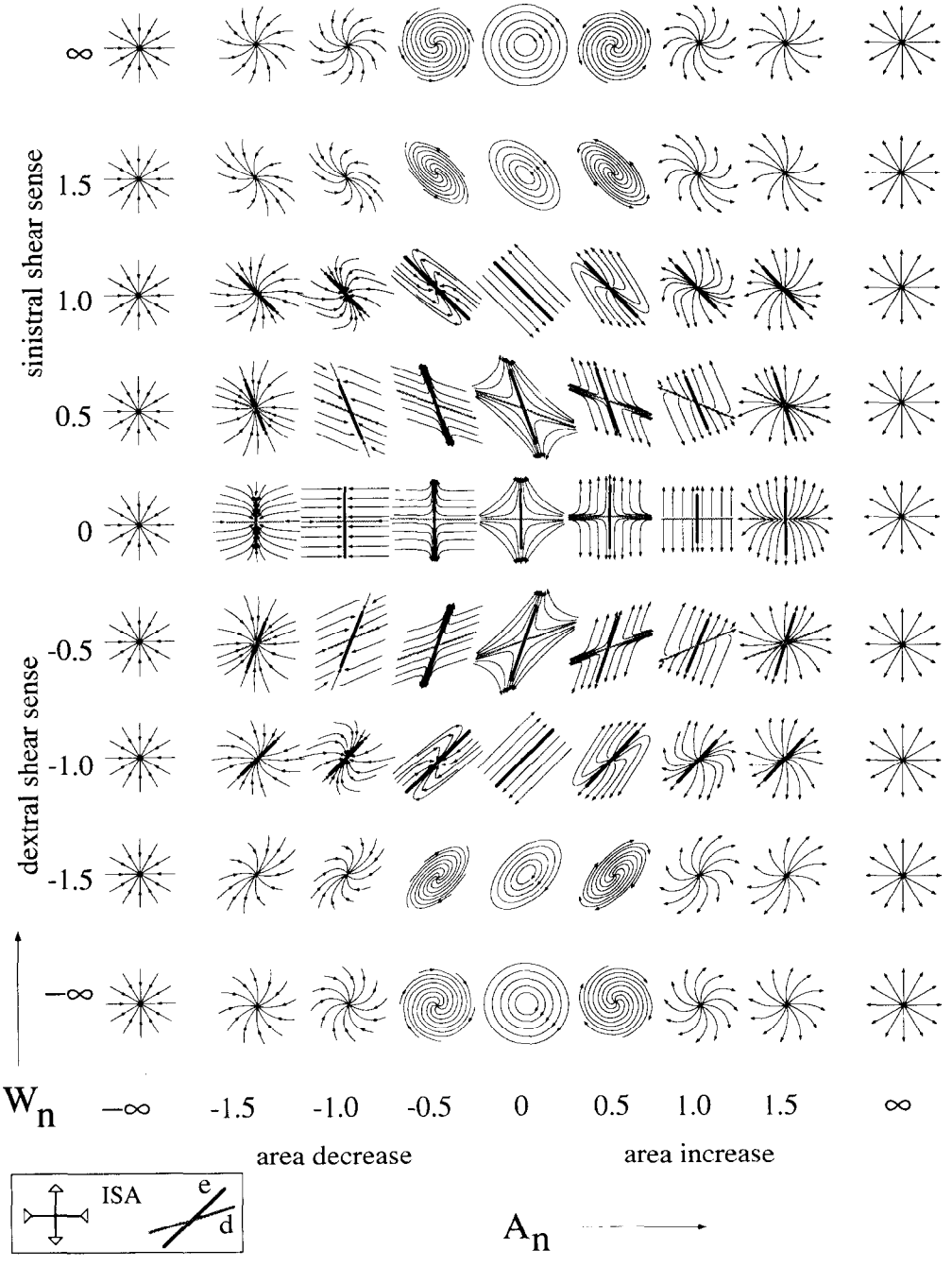

Fig. 3. W_n–A_n plane showing a selection of two-dimensional flow types represented by streamlines. Solid grey and black lines represent flow apophyses **d** and **e**, respectively. Arrows indicate displacement direction of particles in the flow. The orientation of instantaneous stretching axes (ISA) for all flow types is shown in a box.

sive steady-state deformation, with ISA fixed in an external reference frame and no change in flow parameters. The best known flow types are those for $A_n = 0$, such as pure shear ($W_n = 0$), simple shear ($W_n = 1$ or -1) (Fig. 2), general flow or sub-simple shear (DePaor, 1983) ($0 < W_n < 1$ or $-1 < W_n < 0$) and rotational flow or super-simple shear (DePaor, 1983) ($W_n > 1$ or $W_n > -1$); in three dimensions, these flow types are usually defined for plane strain ($T_n = 0$). Notice that all possible two-dimensional homogeneous flow types can be presented in the diagram of Fig. 3, even those in sections other than the *b*–*c* plane; in other planes, however, other sectional kinematic numbers would have to be used for a numeric description.

The following observations can be made from Fig. 3:

(1) Many flow patterns contain one or two straight streamlines through the centre of the diagram. Such straight lines imply that material lines in these orientations do not rotate with respect to the ISA; they coincide

with apophyses **d** and **e** in the *b*–*c* plane (Fig. 1; Ramberg, 1975; Passchier, 1988; Simpson and DePaor, 1993).

(2) The angle α between **d** and **e** depends only on W_n according to:

$$\alpha = \cos^{-1} W_n \tag{8}$$

(Bobyarchick, 1986; Passchier, 1986).

As a result, **d** and **e** can be separate ($-1 < W_n < 1$), joined to a single axis ($W_n = 1$ or $W_n = -1$) or absent ($W_n > 1$ or $W_n < -1$). The A_n–W_n diagram (Fig. 3) can be subdivided vertically according to the number of apophyses; notice that no such simple geometrical subdivision is possible horizontally as a function of A_n.

(3) For all flow types where

$$A_n^2 + W_n^2 = 1, \tag{9}$$

the flow pattern consists exclusively of straight streamlines parallel to **d** or **e** (Fig. 4a). This includes simple shear ($A_n = 0$ and $W_n = 1$ or -1) as a special case. Simple shear is only one of many flow types with straight and parallel streamlines in the *b*–*c* plane (Figs 3 & 4a); other examples are transgression (Tikoff and Teyssier, 1994) and transtension.

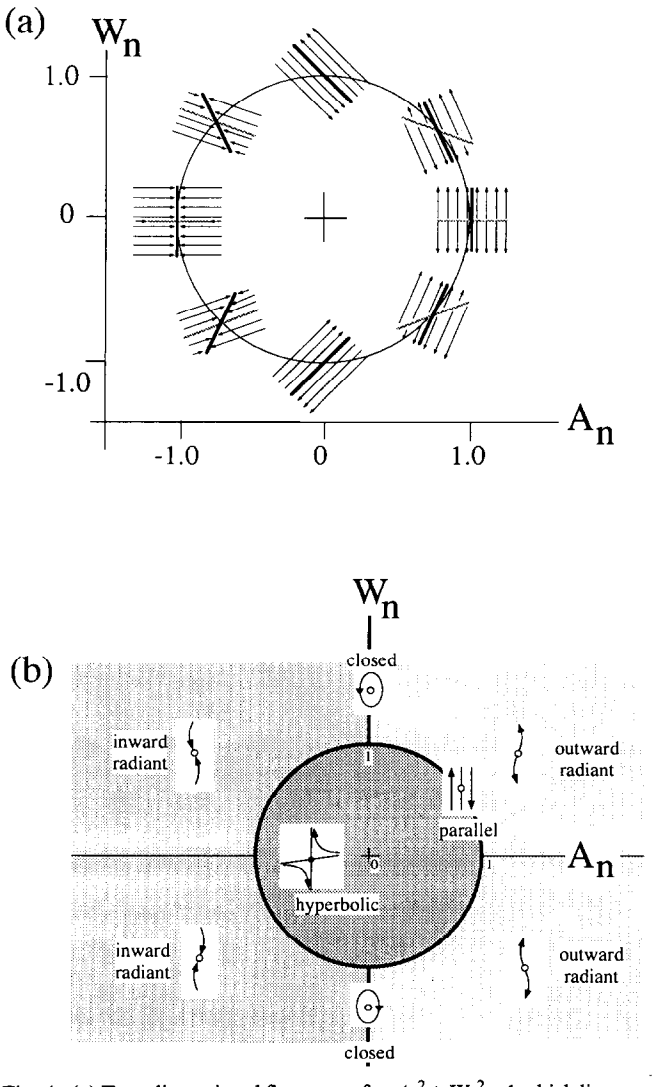

Fig. 4. (a) Two-dimensional flow types for $A_n^2 + W_n^2 = 1$ which lie on a circle in the W_n–A_n plane. These flow types all have one apophysis along which stretching rate is zero, and straight streamlines. (b) General subdivision of two-dimensional flow types according to the shape of their streamline-patterns. Explanation in text.

(4) The circle defined by equation (9) allows a subdivision of flow types into major groups, based on the geometry of the streamlines (Passchier, 1991). Inside the circle, flow types are 'hyperbolic' in shape (Fig. 4b); the streamlines converge on the apophyses as asymptotes but do not reach the centre of the diagram (Ramberg, 1975). On the circle, 'parallel' flow types occur and outside the circle, streamlines are 'radiant' and radiate towards or away from the centre (Figs 3 & 4b); 'inward radiant' and 'outward radiant' directed flow types are separated by 'closed' flow types, consisting of elliptical or circular streamlines (Figs 3 & 4b).

(5) If **d** and **e** are separate apophyses and $b > c$, the stretching rate e of material lines parallel to **e** exceeds the stretching rate d of lines parallel to **d** ($e > d$). For non-dilatant flows ($A_n = 0$) $e = -d$ for $W_n^2 + A_n^2 > 1$ and $A_n > 0$, d and e are positive; for $W_n^2 + A_n^2 > 1$ and $A_n < 0$, d and e are negative;

(6) At very high A_n and W_n, some special flow types occur, and these have been drawn along the edge of the diagram in Fig. 3. These include rigid body rotation ('closed' circular streamlines, $W_n = \infty$) and pure dilation (straight 'radiant' streamlines; $A_n = \infty$) or 'anti-dilation' ($A_n = -\infty$). In the case of pure dilation or anti-dilation, an infinite number of apophyses occur in the *b*–*c* plane; examples are uniaxial constriction, or flattening flow along **a**, and isotropic volume change.

(7) The kinematic vorticity number W_K of Truesdell (1954) changes if A_n or T_n are varied, while W_n remains constant. Since the geometry of flow in the *b*–*c* plane as shown in Fig. 3 depends only on W_n, this seems a more suitable kinematic vorticity number to describe monoclinic flows than W_K.

Because of the large variety of flow types, it is not possible in a single paper to give an outline of the endless variety of different possible deformation paths involving a sequence of different flow types with time. In order to show the effects of flow parameters in progressive deformation, I have therefore chosen to show just some end members of progressive deformation histories, and only those with non-changing flow parameters.

MATERIAL LINE ATTRACTORS

If a homogeneous flow is defined with ISA that are not rotating in the external reference frame, material lines in all orientations will be rotating at a specific angular velocity, except for lines parallel to the flow apophyses. As a consequence, many material lines rotate towards or away from the apophyses (Fig. 5). Three types of apophyses can be distinguished, depending on the move-

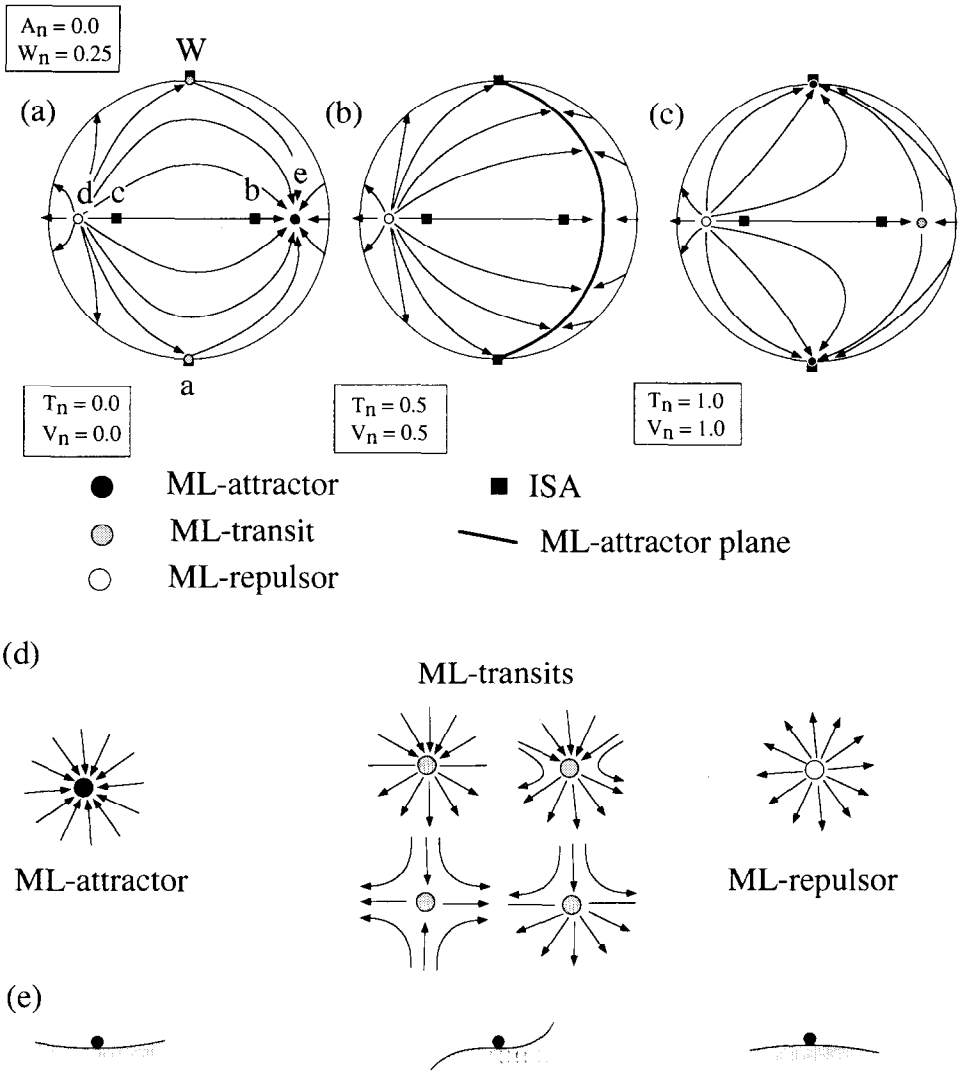

Fig. 5. (a–c) Stereograms representing the rotation of material lines between attractors, transits and repulsors in three monoclinic flow types. (a) Plane strain flow, the apophysis **e** acts as a ML-attractor. (b) Stretching rate along **a** equals that along **e**; an ML-attractor plane exists though **a** and **e**. (c) Stretching rate along **a** exceeds that along **e**; **a** acts as an ML-attractor. (d) Schematic illustration of the concept of ML-attractor, -transit and -repulsor seen at right angles to the apophysis, with relative movement of material lines (arrows). (e) Presentation of three equilibrium states that may serve as analogues for apophysis-types in (d).

ment pattern of material lines at a small angle to these axes: repulsor-, attractor-and transit-apophyses of material lines (abbreviated as 'repulsor', 'attractor' and 'transit' in this paper, Fig. 5). All material lines near a repulsor rotate away from it in all directions; those near an attractor rotate towards it from all directions; and lines near a transit may rotate towards or away from it depending on their orientation. Transits are in fact as much repulsors as attractors (Fig. 5d; Passchier and Trouw, 1995). The principle of attractor-, transit- and repulsor-apophysis classes may be easier to understand if one considers an analogy with the concept of stable-, semi-stable- and unstable-equilibrium in physics, usually illustrated by the behaviour of a sphere on a curved surface (Fig. 5e).

Attractors and transits influence rotation of material lines in different ways. Material lines rotating towards a transit become subparallel to this apophysis, and their further movement is then effectively blocked. However, a small deviation in the flow may cause such blocked lines to rotate into the domain of repulsed lines, after which the line can rotate away from the apophysis (Fig. 5d). In the case of attractors, such small deviations in flow can change the rotational behaviour of material lines at a small angle to the apophysis, but cannot 'push' them away permanently. For practical purposes, however, transits can usually be regarded as a special type of attractor, transitional to repulsors. If deformation is accumulating for some time by the same flow type, material lines will rotate permanently towards an attractor-apophysis and such spatial axes are therefore referred to as *material line* (*ML*) *attractors* (Fig. 5).

Prolate objects such as elongate phenocrysts in a magma, or tourmaline and sillimanite grains in a more

fine-grained flowing matrix may show similar behaviour as material lines; after a certain strain has accumulated, such objects will show a preferred orientation that concentrates near the ML-attractor (Passchier, 1987; Fossen *et al.*, 1994). For oblong objects such as micas or rectangular phenocrysts in a magma, the rotational behaviour is more complex but even these rotate towards parallelism with the ML-attractor (Passchier, 1987). It should be stressed, however, that rigid objects in a ductile matrix will only rotate towards ML-attractors if their axial ratio is high; in other cases, such objects have their own attractors whose orientation also depends on the axial ratio of the object (Passchier, 1987).

In most flow types, attractors and repulsors are lines in space but in some cases, if two of the three flow eigenvalues are equal, attractor-or repulsor *planes* through two of the apophysis positions may exist (Fig. 5b; Passchier, 1987). In such planes each line acts as an attractor or repulsor. In the case of a repulsor plane there is one attractor oblique to the plane; in the case of an attractor plane there is one oblique repulsor (Fig. 5b). In the case of simple shear, a plane of non-rotating lines connects **a** and the joined apophyses **d** and **e**. This plane is also known as the 'flow plane' of simple shear. The joined apophyses **d** and **e** act as an ML-transit and all material lines except those in the irrotational plane rotate towards or away from this **d**/**e**-transit (Passchier, 1987). This transit effectively blocks rotation of material lines in simple shear flow.

Obviously, flow is not likely to remain constant in character with time in any geologically realistic situation. However, if the flow type or orientation of ISA change gradually, the orientation of the ML-attractor will also change proportionally, and attracted material lines or elongate fabric elements will tend to follow the attractor. Therefore, any preferred orientation of elongate objects will track the orientation of the ML-attractor. Obviously, the accuracy by which this position is tracked increases with finite strain.

The concept of attractors and repulsors is not restricted to flows with monoclinic or higher symmetry. The apophyses of triclinic flow can also act as attractors. In monoclinic flows, attractors lie along **a** or in the *b*–*c* plane, but in triclinic flows attractors may have other orientations. Because of the large number of possible geometries, a full analytical approach to attractors in triclinic flows has not been attempted in this study.

Orientation of ML-attractors in monoclinic flow

In monoclinic flow, the position of ML-attractors depends on flow parameters. Material lines tend to rotate towards the apophysis along which the highest stretching rate occurs. In plane strain, stretching rate a along **a** is zero and the apophysis in the *b*–*c* plane with maximum stretching rate, **e**, act as the ML-attractor. This effect is shown in the stereogram in Fig. 5(a). If a is not zero, three situations are possible:

(1) If $a<e$ then **e** is the ML-attractor. a may even be negative, in which case **e** will be an even more effective ML-attractor (Sanderson and Marchini, 1984; Fossen and Tikoff, 1993; Fossen *et al.*, 1994).

(2) If $a=e$ then an ML-attractor plane as discussed above exists through **a** and **e** (Fig. 5b). Material lines rotate towards this plane, but lines within the plane do not rotate. $a=e=d=0$ is the special case of simple shear mentioned above.

The attractor plane through **a** and **e** is not unique; if $b=c$, the *b*–*c* plane acts as an attractor ($a<b$) or repulsor ($a>b$) plane and if $a=d$, the *a*–*d* plane is a repulsor plane.

(3) If $a>e$ then **a** is the ML-attractor (Sanderson and Marchini, 1984; Fossen and Tikoff, 1993; Fig. 5c).

There are thus two possible orthogonal orientations of the ML-attractor in monoclinic flow, but no intermediate orientations except when an ML-attractor plane exists. However, such a plane may be rare in practice. In this paper, the two possible orientations of the ML-attractor are described as **a**ML- and **e**ML- attractors, respectively.

The distribution of **a**ML- and **e**ML- attractors over different flow types can be expressed in terms of W_n, A_n and T_n. The critical value separating **a**ML- and **e**ML-attractors, when an attractor plane exists, is

$$a = e \quad \text{(Fig. 5b)}, \tag{10}$$

or

$$a = \frac{b+c}{2} + \frac{b-c}{2}.\sin\alpha, \tag{10'}$$

which implies that

$$\sin\alpha = \frac{2a-b-c}{b-c} = 2T_n - A_n, \tag{11}$$

and since

$$\sin\alpha = \sqrt{1 - W_n^2} \tag{12}$$

(Passchier, 1988);

$$2T_n - A_n = W_d \tag{13}$$

(cf. Passchier, 1987); where

$$W_d = \sqrt{1 - W_n^2} \tag{14}$$

(Passchier, 1988).

Equation (13) can also be given in terms of normalised volume change rate using equation (7) as;

$$2V_n - 3A_n = W_d, \tag{15}$$

or

$$3T_n - V_n = W_d. \tag{16}$$

Notice that for plane strain flow ($T_n=0$),

$$W_d = -A_n = -V_n \tag{17}$$

and for isochoric flow ($V_n = 0$):

$$W_d = -3A_n = 3T_n \tag{18}$$

Figure 6 shows a three dimensional graph for W_n–A_n–T_n space in which any monoclinic flow type can be plotted as a point. This diagram shows the distribution of flow types that lead to development of **a**ML- and **e**ML-attractors through progressive deformation with invariable flow parameters; the oblique cylinder-surface separates domains of **a**ML- and **e**ML-attractors, based on Eq. (13). The curved line on the cylinder-surface is the intersection with the plane of isochoric flow types ($V_n = 0$; $T_n = -A_n$). The following conclusions can be drawn from Fig. 6 and from Eq. (13):

(1) If $T_n = 0$ (plane strain flow), an **e**ML-attractor exists for any W_n value if $A_n > 0$; this would imply instantaneous volume increase ($V_n > 0$; Fig. 2). If $A_n < 0$ (instantaneous volume decrease; $V_n < 0$; Fig. 2), an **e**ML-attractor exists at low W_n-values up to a limit described by equation (17). However, at $A_n < -1$ an **a**ML-attractor exists for all W_n values. Notice that at $A_n = 0$ and $W_n = 1$ or -1 (simple shear), small deviations in A_n, W_n or T_n can cause development of an **a**ML-attractor instead of the **e**ML-transit of simple shear (Fig. 6). Simple shear is extremely sensitive to small deviations from ideal conditions. Other non-coaxial flow types at lower W_n values, will have **e**ML-attractors except at extreme deviations in T_n or A_n.

(2) If $T_n < 0$ (Figs 2 & 6), an **e**ML-attractor exists except at very low A_n values, which are probably never attained in rocks.

(3) If $T_n > 0$, the conditions at which an **e**ML- or **a**ML-attractor can be reached are complicated and described by Eq. (13).

ATTRACTORS OF FINITE STRAIN AXES

Most fabrics in rocks reflect the orientation of finite strain axes rather than the preferred orientation of material lines. Analogous to material lines, the principal axes of the finite strain ellipsoid also tend to rotate towards attractors (e.g. Ramsay and Huber, 1983). This is most obvious when the behaviour of the X-axis of finite strain is considered, which commonly defines the orientation of mineral and stretching lineations and many foliations in rocks.

The accumulation of finite strain is a function of the flow parameters discussed above. For $0 \leq W_n < 1$ monoclinic flow can be described by a flow tensor **L**;

$$\mathbf{L} = \begin{bmatrix} a & 0 & 0 \\ 0 & \frac{b+c}{2} & \frac{b-c}{2}(1+W_n) \\ 0 & \frac{b-c}{2}(1-W_n) & \frac{b+c}{2} \end{bmatrix} = \begin{bmatrix} 2T_n\dot{s} & 0 & 0 \\ 0 & A_n\dot{s} & \dot{s}+W_n\dot{s} \\ 0 & \dot{s}-W_n\dot{s} & A_n\dot{s} \end{bmatrix}, \tag{19}$$

where $\dot{s}$ is the stretching rate defined in Eq. (1). **L** can be used to derive a finite position gradient tensor $\mathbf{F_f}$ at a time t, accumulated by progressive deformation at constant, invariable flow parameters following Ramberg (1975), McKenzie (1979) and Passchier (1988):

$$F_f = \begin{bmatrix} \exp(2T_nS_t) & 0 & 0 \\ 0 & \exp(A_nS_t)\cosh(W_dS_t) & \frac{\exp(A_nS_t)(1+W_n)}{W_d}\sinh(W_dS_t) \\ 0 & \frac{\exp(A_nS_t)(1-W_n)}{W_d}\sinh(W_dS_t) & \exp(A_nS_t)\cosh(W_dS_t) \end{bmatrix} \tag{20}$$

where

$$S_t = \dot{s}t. \tag{21}$$

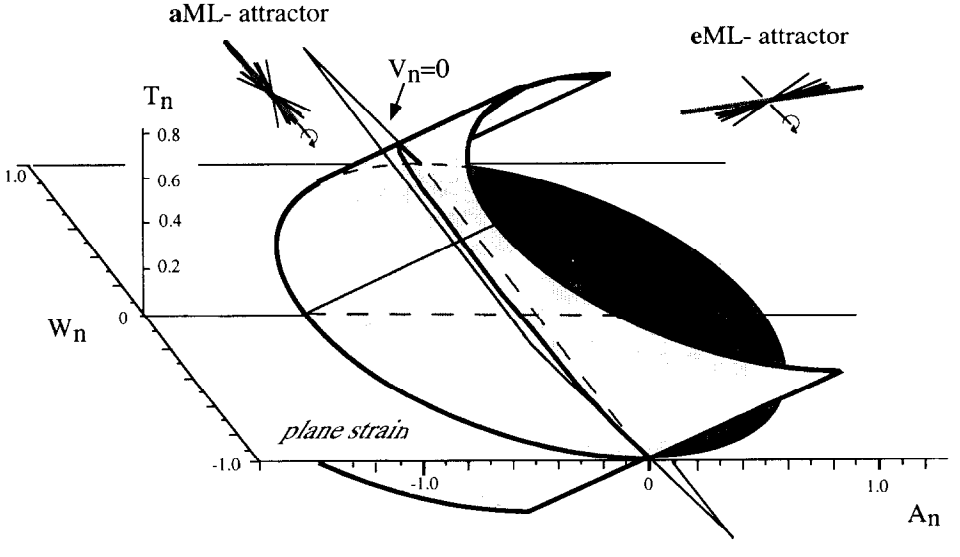

Fig. 6. W_n–A_n–T_n space showing the distribution of flow types with an ML-attractor along **a** (left) and **e** (right). A cylindrical surface separates the domains. The arc on the cylindrical surface represents its intersection with the plane of isochoric flow types ($V_n = 0$ or $T_n = -A_n$; no volume change). Each type of monoclinic flow can be presented by a point in this W_n–A_n–T_n diagram.

S_t, the product of stretching rate and time, is a useful dimensionless number which serves as a universal measure of strain at a certain stage of progressive deformation, regardless of the type of deformation path.

If $0 \leq W_n < 1$ Eq. (20) can be rewritten in terms of principal finite strains (stretch values) as (Passchier, 1988):

$$s_1 = \exp(2T_n S_t), \tag{22}$$

$$s_2 = \frac{\exp(A_n S_t)}{W_d}\left\{\sinh(W_d S_t) + \sqrt{(\cosh^2(W_d S_t) - W_n^2)}\right\}, \tag{23}$$

$$s_3 = -\frac{\exp(A_d S_t)}{W_d}\left\{\sinh(W_d S_t) - \sqrt{(\cosh^2(W_d S_t) - W_n^2)}\right\}; \tag{24}$$

and for $W_n = 1$:

$$s_1 = \exp(2T_n S_t), \tag{25}$$

$$s_2 = \exp(A_n S_t)\left\{S_t + \sqrt{1 + S_t^2}\right\}, \tag{26}$$

$$s_3 = -\exp(A_n S_t)\left\{S_t - \sqrt{1 + S_t^2}\right\}. \tag{27}$$

By definition, s_1 accumulates along **a**, while s_2 and s_3 lie in the *b*–*c* plane. Notice that 1, 2 and 3 refer to directions, not relative magnitudes of the principal finite strains.

The orientation of an *X*-attractor depends on the relative magnitudes of s_1, s_2 and s_3. s_2 rotates from the position of **b** at infinitesimally small strain towards **e**. However, **e** only acts as an *X*-attractor if s_2 is the longest finite strain axis (**e***X*-attractor); if s_1 is the longest axis, **a** will be the *X*-attractor (**a***X*-attractor). The boundary between an **a***X*- and **e***X*-attractor lies at $s_1 = s_2$.

Using a spreadsheet, the accumulation of progressive deformation can be calculated using the equations (22)–(27), and the transition from $s_1 > s_2$ to $s_1 < s_2$ can be determined. This leads to the following results:

(1) At $W_n = 0$, the result depends on the magnitudes of *a*, *b* and *c*: strain simply accumulates fastest along the axis with highest stretching rate, either **a** (**a***X*-attractor; *X* accumulates parallel to a) or the combined axis **b** = **e** (**e***X*-attractor; *X* accumulates parallel to **b** = **e**).

(2) At $0 < W_n \leq 1$ or $-1 \leq W_n < 0$, the result depends on the magnitude of **a**. If $a \leq 0$ in all stages of progressive deformation then an **e***X*-attractor exists (Fig. 7a). If $a > 0$, the situation is more complicated. Pfiffner and Ramsay (1982) have shown that finite strain accumulates more slowly in simple shear than in pure shear at similar instantaneous stretching rates. This means that, if $0 < a < b$, s_2 can initially exceed s_1 but this situation may

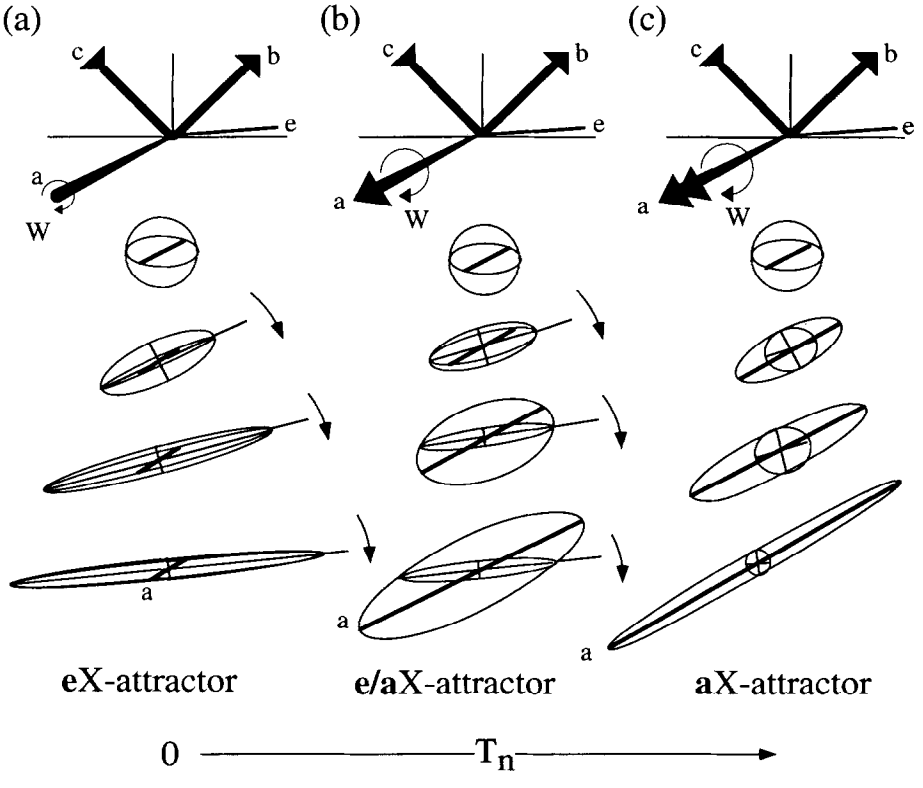

Fig. 7. The three classes of development of finite strain ellipsoids with respect to *X*-attractors in progressive deformation by monoclinic flow, shown for three different T_n values and similar W_n. (a) **e***X*-attractor; in plane strain ($T_n = 0$), the *X*-axis rotates towards **e**. (b) **e**/**a***X* attractor; at a small T_n, *X* may first rotate towards **e**, then accumulate along **a**. (c) **a***X*-attractor; at high T_n, *X* accumulates along **a** throughout the deformation history. The bold line in ellipsoids is parallel to **a**.

reverse during progressive deformation since strain accumulates most rapidly along **a** (Fossen and Tikoff, 1993; Tikoff and Teyssier, 1994; Fig. 7b); this attractor 'swapping' is referred to here as **e**/**a**X-attractor. Only if $a > b$, $s_1 > s_2$ in all stages of progressive deformation and an **a**X-attractor always exists (Fossen and Tikoff, 1993; Fig. 7c). The limiting condition $a = b$ can be rewritten in terms of kinematic numbers as;

$$2T_n - A_n = 1, \tag{28}$$

and this is the equation separating domains of **e**/**a**X- and **a**X-attractors. In terms of V_n:

$$3T_n - V_n = 1, \tag{29}$$

and

$$2V_n - 3A_n = 1. \tag{30}$$

Figure 8 is a W_n–A_n–T_n diagram similar to Fig. 6 in which two surfaces separate domains of flow types that lead to development of **a**X-, **e**/**a**X- and **e**X-attractors through progressive deformation with invariable flow parameters. The planar surface represents Eq. (28) and separates domains of **a**X- and **e**/**a**X-attractors. The curved surface (as in Fig. 6) separates the **e**/**a**X- from the **e**X-attractor domain and represents Eq. (13).

Small deviations from ideal simple shear in a ductile shear zone (Fig. 8) may cause development of an **a**X-attractor at high strain rather than the expected **e**X-transit of simple shear, since flow shifted to the **e**/**a**X-attractor domain.

APPLICATION OF THE ATTRACTOR CONCEPT

The concept of attractors of material lines or of the X-axis of finite strain as described above can be used in studies of flow and fabric development in rocks, especially in high-strain rocks and for modelling using non-standard flow types. In the following section, the attractor concept is applied to some aspects of structural geology in order to illustrate how it may be used.

Transpressive shear zones

Flow in model transpressive shear zones (Harland, 1971) is volume constant, and thinning of the shear zone is compensated by extension parallel to **a** and **w**; no stretch occurs along the shear zone boundary in the b–c plane of flow (Sanderson and Marchini, 1984; Fossen and Tikoff, 1993; Robin and Cruden, 1994; Krantz, 1995). Transpressive shear zones plot in the $V_n = 0$ plane, which is a cross-section through Fig. 8 shown in Fig. 9(a). Transpressive shear zones plot on the circle where $W_n^2 + A_n^2 = 1$, and lie in both the **e**/**a**X- or **a**X-attractor fields (Fig. 9a, TP). At high strain, such zones therefore inevitably develop with X (and therefore stretching lineations) parallel to **a** and **w** (Fig. 9b). This means that asymmetric structures, used to determine sense of shear, will be found on outcrop surfaces *normal* to the stretching lineation, and not on surfaces parallel to the lineation as for shear zones with simple shear flow (Fig. 9b). Examples of such unusual shear zones have been described from Canada (Hudleston *et al.*, 1988; McDonough and Simony, 1989; Robin and Cruden, 1994), Sweden (Robin and Cruden, 1994; Talbot and Sokoutis, 1995) and NE-Spain (Carreras and Druguet, 1994). The diagram of Fig. 8 can also be used to predict the behaviour of shear zones other than simple shear or transpression, and at $V_n \neq 0$. For example, at $V_n = 1$ or $V_n = -1$, the circle of 'transpression' flow lies completely in the **e**X- or **a**X-fields (Fig. 9c).

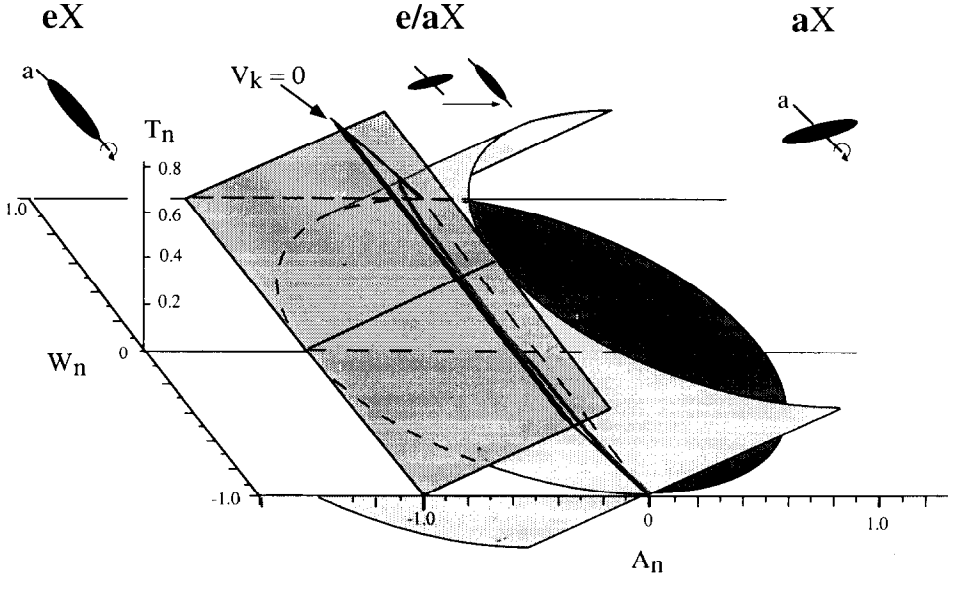

Fig. 8. W_n-A_n-T_n space showing the distribution of flow types that lead to an **a**X-attractor (left), an **e**X-attractor (right) and a transitional domain with **e**/**a**X-attractor (centre), provided that deformation proceeds by time-independent flow. The cylindrical surface that separates **e**/**a**X- and **e**X-domains is similar to that in Fig. 6. Bold lines on the limiting surfaces represent their intersection with the plane of isochoric flow ($V_n = 0$ or $T_n = -A_n$: no volume change).

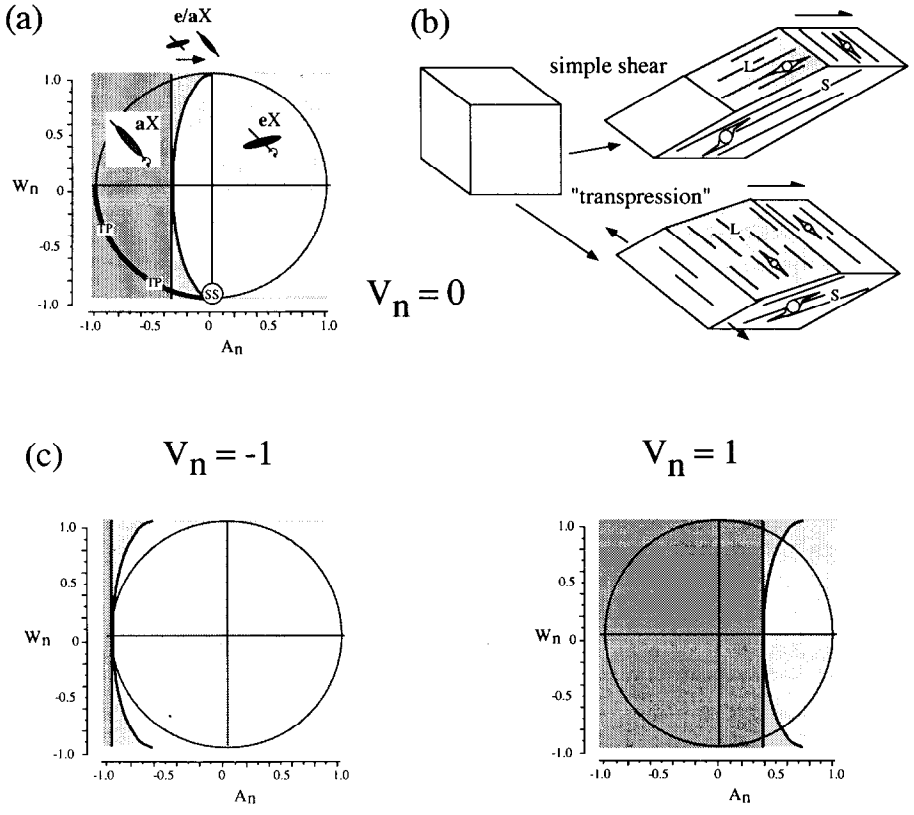

Fig. 9. (a) Cross-section through Fig. 8 for $V_n = 0$. Three-dimensional flow types can be plotted as points in this plane and the geometry of flow and finite deformation depends on W_n and A_n (or T_n). Three fields of increasing shading are domains of **e***X*-, **e**/**a***X*- and **a***X*-attractors. The position of flow types in simple shear (SS) and transpression (TP) shear zones is indicated (only shown for dextral shear sense as illustrated in (b)). Transpression flow types lie in the **a***X*-and **e**/**a***X*-fields, and develop stretching lineations parallel to the vorticity vector at high strain. (b) Fabric development in simple shear and transpression; transpression is shown with a horizontal vorticity axis for convenience. *S*-foliation; *L*-stretching lineation. A foliation plane is indicated in grey. (c) Cross-sections of Fig. 8 for two types of instantaneous volume increase ($V_n = 1$) and decrease ($V_n = -1$).

Attractor-meshes

The attractor concept can be particularly useful in studies or models of heterogeneous deformation. For this application, attractors should not be treated as isolated straight lines, but as a mesh of curved lines in space, as explained below.

Lineations are usually presented on maps and drawings as isolated lines of a specific orientation. In reality, they form a mesh of subparallel linear structures in the rock with a complex three-dimensional shape. This mesh may change laterally in orientation, be folded, or bend around rigid objects. In a similar way magnetic field lines, principal stress axes and ISA can be envisaged to form different meshes of lines inside a volume of material. A distinction may be made between *permanent* meshes such as that of different types of lineations, which can actually be sampled and measured in a rock and *transient* meshes such as that of stress axes or ISA which can be imagined to exists temporarily during progressive deformation. Transient meshes can shift through a volume of material; permanent meshes are fixed in the rock and can only change shape by deformation. Finite strain axes and material lines form separate permanent meshes since they do not remain parallel during non-coaxial progressive deformation.

ML-or *X*-attractors as described in the previous sections can be imagined as being arranged in a transient mesh that is present in deforming rocks. Ductile deformation can be regarded as a permanent attempt of the meshes of material lines and strain axes to adapt to the shape of the attractor-mesh; only in time-independent pure shear flow do these meshes coincide throughout the deformation history; in non-coaxial flow histories, the meshes of material lines and strain axes will only approach parallelism with the attractor-mesh at high finite strain. The attractor-mesh is in its turn related to the stress mesh, their degree of coincidence depending on the rheology and anisotropy of the rock and lateral variations therein.

The concept of an attractor-mesh can also help to model development of structures formed by inhomogeneous flow. The next paragraphs serve to illustrate the concept.

Application of the attractor-mesh concept

In the case of homogeneous non-coaxial flow and progressive deformation with non-variable parameters,

the attractor-mesh consists of straight parallel lines. Material lines and finite strain axes attracted to the lines of such an attractor-mesh will also form straight lineations and planar foliations, which will approach parallelism with the attractor-mesh at high finite strain. Such 'straight' fabrics are found in the core of medium-to high-grade shear zones, which may represent a regime where attractor-meshes of this type are common.

Slightly more complex is the situation in shear zones with deforming wall rocks, such as stretching shear zones. A stretching shear zone (Means, 1989) is a plane-strain shear zone with wall rocks that undergo ductile extension during non-coaxial flow in the zone (Fig. 10). Flow in such a stretching shear zone is non-coaxial with $0 < W_n < 1$ or $-1 < W_n < 0$ and plots along the $A_n = 0$ and $T_n = 0$ axis in the diagram of Fig. 8.

Imagine a simple model of a stretching shear zone with coaxial progressive deformation in the wall rock (Fig. 10). Both in the shear zone and in the wall rock, **e** is parallel to the shear zone boundary and acts as both an **e***ML*-and **e***X*-attractor. The attractors can be imagined to form a mesh of lines in the rock parallel to the shear zone boundary (Fig. 10). Material lines and the *X*-axis of strain rotate towards the attractor-mesh in the shear zone, and accumulate along it in the wall rock (Fig. 10). The result is in an inward-steepening fabric gradient, which will evolve into a fabric subparallel to the attractor-mesh (and thus to the shear zone boundary) at high finite strain.

In heterogeneous flow and progressive deformation, the attractor-mesh may be visualised as being bent in a complex way, and this geometry will change with time. Although material lines will be attracted to the mesh, it is difficult to predict what the final fabric will look like. In many cases, the fabric may mimic the irregular shape of the attractor-mesh. As a simple example, consider an elongate rigid boudin in non-coaxial flow: the attractor-mesh will wrap around the boudin, and foliations and lineations that develop at this site will consequently be curved (Fig. 11).

An interesting curiosity is that attractor-meshes may locally develop 'holes', where no attractor is present. This is probably most common for transit-meshes such as in the case of simple shear. Consider a simple shear zone in which flow is slightly inhomogeneous in the sense that the rotation component of flow is not constant over the zone (Simpson and DePaor, 1993; Fig. 12). Locally, transient domains occur where W_n is either smaller or larger than 1. Where $W_n < 1$, the 'transit-mesh' grades into an attractor-mesh and is simply continuous, but where $W_n > 1$, it is interrupted, since under such conditions no apophysis is present in the *b*–*c* plane (Figs 3 & 12; DePaor, 1983; Passchier, 1988). In the 'hole', material lines can rotate beyond the orientation of the transit in the surrounding mesh, and folds develop as a consequence: this may be an important cause for the development of sheath folds in mylonites developed in simple shear (Hudleston, 1976; Vollmer, 1988). In shear zones with a lower W_n and **e** parallel to the shear zone boundary (Coward, 1976; Ramsay, 1980; Kligfield *et al.*, 1981; Paterson and Waingler, 1991) an attractor-mesh rather than a transit-mesh is present; a 'hole' is less likely to develop in such an attractor-mesh since much larger fluctuations in W_n are necessary. On theoretical grounds, it is therefore less likely that shear folds develop in low-W_n shear zones.

Another possible site where holes or deflections in an attractor- or transit-mesh occur is near a rotating rigid object in non-coaxial flow (Fig. 13). At some distance from the object, the mesh is curved but continuous, and this causes curving of foliations and lineations near the object; at high strain the fabric will mimic the shape of the

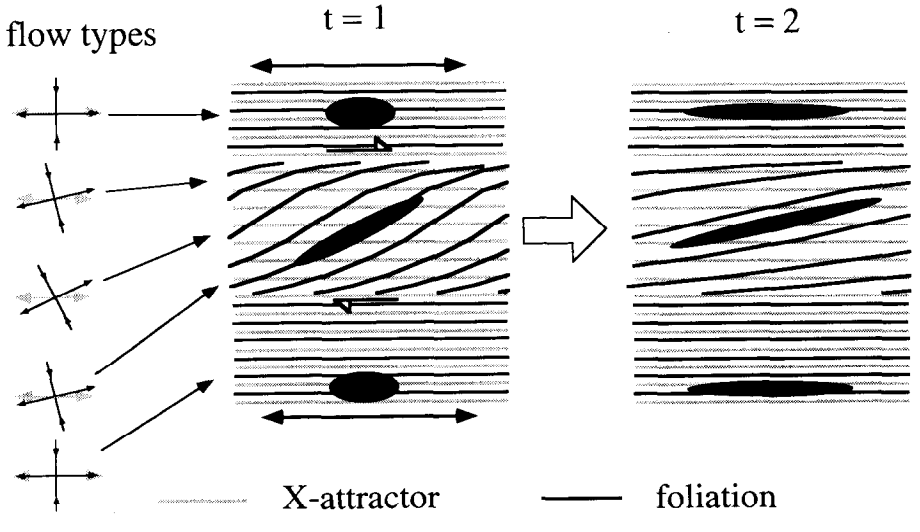

Fig. 10. Two stages in the development of a stretching shear zone illustrating the concept of an attractor-mesh. Flow types in the wall rock and the shear zone are illustrated at left by ISA (bold black arrows) and the attractor apophysis **e** (grey arrow). Grey lines in the diagrams at right represent the attractor-mesh; black lines represent the developing shape fabric. The shape fabric develops parallel to the attractor-mesh in the wall rock, but rotates towards the mesh in the shear zone.

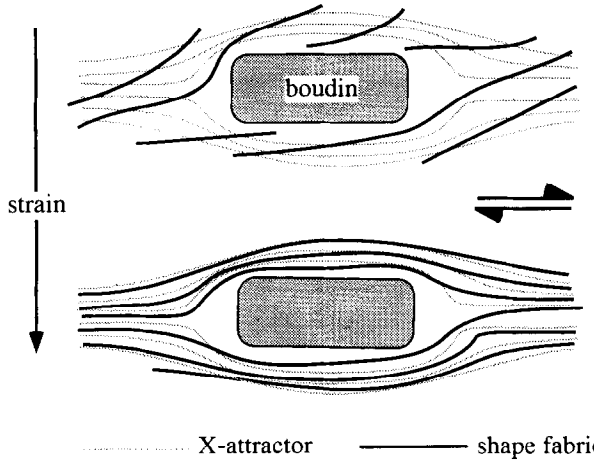

Fig. 11. Flow around a rigid boudin may define a curved attractor-mesh (grey lines) which governs the development of the shape fabric (black lines). At high strain, the shape fabric mimics the shape of the attractor-mesh.

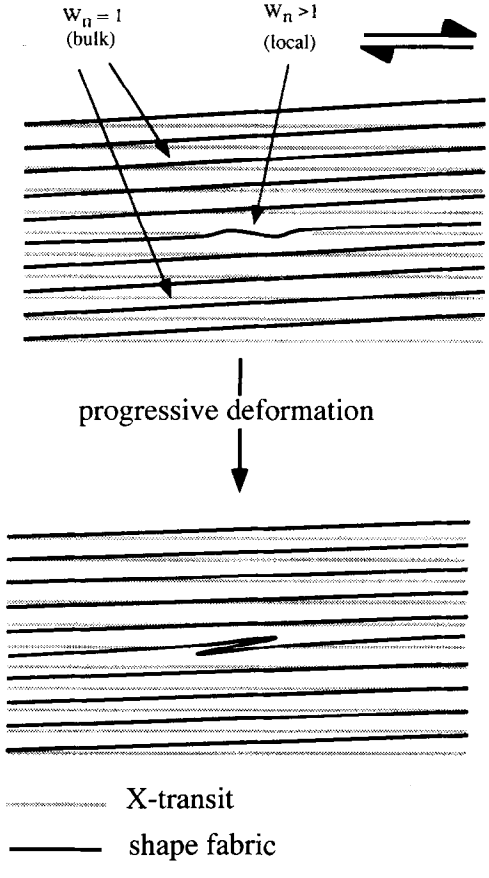

Fig. 12. Development of a sheath fold in simple shear. The transit-mesh of simple shear (grey lines) is interrupted at one spot where flow has a W_n value > 1. At this point, the shape fabric (black lines) can rotate "through" the orientation of the mesh, and develop sheath folds.

curved attractor (Passchier, 1994). Immediately adjacent to the rigid object, however, a mesh of elliptical lines exists which is not continuous with the external mesh. Here, material lines can wrap around the object indefinitely. This may be the cause of the development of δ-objects and quarter folds (Hanmer and Passchier, 1991; Simpson and DePaor, 1993; Passchier and Trouw, 1995; Fig. 13).

Kinematic analysis using attractors

Since shape fabrics and elongate objects rotate towards parallelism with attractors at high strain, the orientation of such fabric elements can be used in high-strain zones to determine the approximate orientation of attractors, or even attractor-meshes. Since attractors are part of the kinematic frame of flow, flow parameters such as W_n, T_n and A_n can theoretically be deduced from rock fabrics if the orientation of additional elements of the kinematic frame can be found. T_n and A_n can be determined from volume change and three-dimensional strain data. The geometry of fibre aggregates (Passchier and Trouw, 1995) can be used to determine the orientation of ISA with respect to the attractor and, since W_n defines the angle between ISA and the attractor, these data could be used to find W_n. Such analyses may give relevant results if flow was monoclinic and if flow geometry did not change much during progressive deformation. In other cases, fibre trajectory analysis (Fisher and Anastasio, 1994; Passchier and Trouw, 1995) may help to determine flow evolution.

Fabric attractors

Flow apophyses may serve as attractors of material lines or finite strain axes, but other fabric elements have also been reported to show a specific preferred orientation with respect to elements of the kinematic frame. Some examples are: the central girdles of quartz crystallographic fabrics that seem to be fixed orthogonal to the ML-attractor (Lister and Hobbs, 1980; Schmid and Casey, 1986), probably because crystal slip planes rotate towards the attractor (Passchier and Trouw, 1995); oblique foliations which make a small but fixed angle with ISA (Means, 1981; Passchier and Trouw, 1995); and C-planes in a C–S fabric which seem to be fixed parallel to an ML-attractor or transit (Berthé *et al.*, 1979; Lister and Snoke, 1984). All these fabric elements have an orientation that is independent of finite strain, although the strength of the fabric increases with finite strain. It is therefore possible to classify them as fabric elements that accumulate near some kind of attractor: a general concept of *fabric attractors* can be defined, the nature and orientation of which depends on the type of fabric concerned (Passchier and Trouw, 1995). For example, a subdivision of foliations may be possible into those that approach an attractor, those which are fixed to an attractor and those that are independent. In this paper, treatment is restricted to ML- and X-attractors.

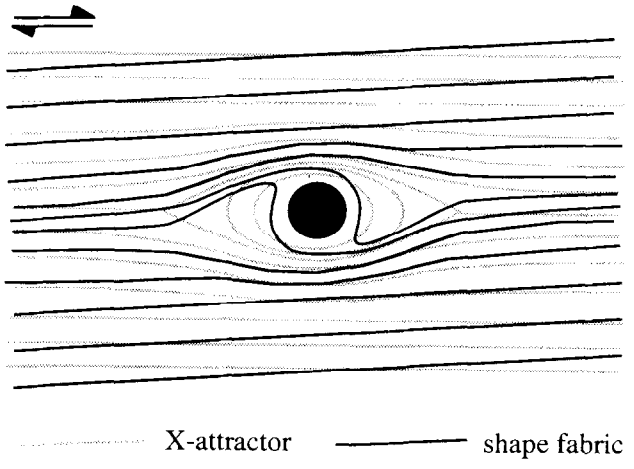

Fig. 13. Deformation around a spherical rigid object in non-coaxial flow. The attractor-mesh (grey lines) is deflected near the sphere, and consists of isolated elliptical scales adjacent to the sphere. The developing shape fabric (black lines) near the sphere rotates around the sphere within the elliptical mesh-segment.

CONCLUSIONS

Three dimensional flow in shear zones is thought to be approximately monoclinic. Any type of monoclinic flow can be fully expressed by three numbers, W_n, A_n and T_n which determine the nature and orientation of flow apophyses. Flow apophyses can be divided into attractors, transits and repulsors of material lines, principal finite strain axes and crystal slip planes. Foliations and lineations can be expected to accumulate near attractors and an understanding of the nature and orientation of attractors in deforming rocks can be of use for modelling and studies of fabric development. Examples are the development of lineations parallel to the vorticity vector in transpressive shear zones, and the development of sheath folds and mantled porphyroclasts or boudins. The concept of attractors is an alternative way to look at the accumulation of fabrics in rocks, and allows a better integration of flow modelling and fabric analysis in tectonic studies.

Acknowledgements—Critical reviews by Win Means and Basil Tikoff helped to improve this paper and are gratefully acknowledged.

REFERENCES

Berthé, D., Choukroune, P. and Jegouzo, P. (1979) Orthogneiss, mylonite and non-coaxial deformation of granites: the example of the South Armorican shear zone. *Journal of Structural Geology* **1**, 31–42.

Bobyarchick, A. R. (1986) The Eigenvalues of steady flow in Mohr space. *Tectonophysics* **122**, 35–51.

Carreras, J. and Druguet, E. (1994) Structural zonation as a result of inhomogeneous non-coaxial deformation and its control on syntectonic instrusions: an example from the Cap de Creus area, eastern Pyrenees. *Journal of Structural Geology* **16**, 1525–1534.

Coward, M. P. (1976) Strain within ductile shear zones. *Tectonophysics* **34**, 181–197.

DePaor, D. C. (1983) Orthographic analysis of geological structures; 1: Deformation theory. *Journal of Structural Geology* **5**, 255–277.

Fisher, D. M. and Anastasio, D. J. (1994) Kinematic analysis of a large-scale leading edge fold, Lost River Range, Idaho. *Journal of Structural Geology* **16**, 337–354.

Fossen, H. (1993) Linear fabrics in the Bergsdalen nappes, southwest Norway: implications for deformation history and fold development. *Norsk Geologisk Tidsskrift* **73**, 95–108.

Fossen, H. and Tikoff, B. (1993) The deformation matrix for simultaneous simple shearing, pure shearing and volume change, and its application to transpression transtension tectonics. *Journal of Structural Geology* **15**, 413–422.

Fossen, H., Tikoff, B. and Teyssier, C. (1994) Strain modeling of transpressional and transtensional deformation. *Norsk Geologisk Tidsskrift* **74**, 134–145.

Hanmer, S. and Passchier, C. W. (1991) Shear sense indicators: a review. *Geological Survey of Canada, Paper 90*, 117.

Harland, W. B. (1971) Tectonic transpression in Caledonian Spitzbergen. *Geological Magazine* **108**, 27–42.

Hudleston, P. J. (1976) Recumbent folding in the base of the Barnes Ice Cap, Baffin Island, Northwest Territories, Canada. *Bulletin of Geological Society America* **87**, 1684–1692.

Hudleston, P. J., Schultz-Ela, D. and Southwick, D. L. (1988) Transpression in an Archean greenstone belt, northern Minnesota. *Canadian Journal of Earth Science* **25**, 1060–1068.

Kligfield, R., Carmignani, L. and Owens, W. H. (1981) Strain analysis of a northern Appenine shear zone using deformed marble breccias. *Journal of Structural Geology* **3**, 421–436.

Krantz, R. W. (1995) The transpressional strain model applied to strike-slip, oblique-convergent and oblique-divergent deformation. *Journal of Structural Geology* **17**, 1125–1137.

Lister, G. S. and Hobbs, B. E. (1980) The simulation of fabric development during plastic deformation and its application to quartzite—the influence of deformation history. *Journal of Structural Geology* **2**, 355–371.

Lister, G. S. and Snoke, A. W. (1984) *S-C* Mylonites. *Journal of Structural Geology* **6**, 617–638.

Lister, G. S. and Williams, P. F. (1983) The partitioning of deformation in flowing rock masses. *Tectonophysics* **92**, 1–33.

Malvern, L. (1969) *Introduction to the Mechanics of a Continuous Medium*. Prentice-Hall, Englewood Cliffs, New Jersey.

McDonough, M. R. and Simony, P. S. (1989) Valemount strain zone: A dextral oblique-slip thrust system linking the Rocky Mountain and Omineca belts of the southeastern Canadian Cordillera. *Geology* **17**, 237–240.

McKenzie, D. (1979) Finite deformation during fluid flow. *Geophysics Journal of the Royal Astronomical Society* **58**, 689–715.

Means, W. D., Hobbs, B. E., Lister, G. S. and Williams, P. F. (1980) Vorticity and non-coaxialty in progressive deformations. *Journal of Structural Geology* **2**, 371–378.

Means, W. D. (1981) The concept of steady-state foliation. *Tectonophysics* **78**, 179–199.

Means, W. D. (1989) Stretching faults. *Geology* **17**, 893–896.

Passchier, C. W. (1986) Flow in natural shear zones—the consequences of spinning flow regimes. *Earth and Planetary Science Letters* **77**, 70–80.

Passchier, C. W. (1987) Stable positions of rigid objects in non-coaxial flow—a study in vorticity analysis. *Journal of Structural Geology* **9**, 679–690.

Passchier, C. W. (1988) The use of Mohr circles to describe non-coaxial progressive deformation. *Tectonophysics* **149**, 323–338.

Passchier, C. W. (1990) Reconstruction of deformation and flow parameters from deformed vein sets. *Tectonophysics* **180**, 185–199.

Passchier, C. W. (1991) The classification of dilatant flow types. *Journal of Structural Geology* **13**, 101–104.

Passchier, C. W. (1994) Mixing in flow perturbations: a model for development of mantled porphyroclasts in mylonites. *Journal of Structural Geology* **16**, 733–736.

Passchier, C. W. and Trouw, R. A. J. (1995) *Microtectonics*. Springer Verlag, Heidelberg.

Paterson, S. R. and Waingler, L. (1991) Strains and structures associated with a terrane bounding stretching fault: the Melones fault zone, central Sierra Nevada, California. *Tectonophysics* **194**, 69–90.

Pfiffner, O. A. and Ramsay, J. G. (1982) Constraints on geological strain rates—arguments from finite strain states of naturally deformed rocks. *Journal of Geophysical Research* **87**, 311–321.

Ramberg, H. (1975) Particle paths, displacement and progressive strain applicable to rocks. *Tectonophysics* **28**, 1–37.

Ramsay, J. G. (1980) Shear zone geometry: a review. *Journal of Structural Geology* **2**, 83–101.

Ramsay, J. G. and Huber, M. I. (1983) *The Techniques of Modern Structural Geology*, Vol I. Academic Press.

Robin, P. Y. F. and Cruden, A. R. (1994) Strain and vorticity patterns in ideally ductile transpression zones. *Journal of Structural Geology* **16**, 447–466.

Sanderson, D. J. and Marchini, R. D. (1984) Transpression. *Journal of Structural Geology* **6**, 449–549.

Schmid, S. M. and Casey, M. (1986) Complete fabric analysis of some commonly observed quartz c-axis patterns. *Geophysical Monograph* **36**, 263–286.

Simpson, C. and DePaor, D. G. (1993) Strain and kinematic analysis in general shear zones. *Journal of Structural Geology* **15**, 1–20.

Talbot, C. J. and Sokoutis, D. (1995) Strain ellipsoids from incompetent dykes: application to volume loss during mylonitization in the Singö gneiss zone, central Sweden. *Journal of Structural Geology* **17**, 927–948.

Tikoff, B. and Teyssier, C. (1994) Strain and fabric analyses based on porphyroclast interaction. *Journal of Structural Geology* **16**, 477–492.

Truesdell, C. (1954) *The Kinematics of Vorticity*. Indiana University Press, Bloomington.

Vollmer, F. W. (1988) A computer model of sheath nappes formed during crystal shear in the Western gneiss Region, central Norwegian Caledonides. *Journal of Structural Geology* **10**, 735–743.

Weijermars, R. (1991) The role of stress in ductile deformation. *Journal of Structural Geology* **13**, 1061–1078.